Letter

Microfluidic droplet pinch-off modified by hard and soft colloids: A scaling transition

Loïc Chagot,* Simona Migliozzi, and Panagiota Angeli
ThAMeS Multiphase, Department of Chemical Engineering, University College London WC1E 7JE, United Kingdom

(Received 21 March 2024; accepted 6 May 2024; published 28 May 2024)

This Letter explores the influence of colloids at liquid-liquid interfaces on droplet pinch-off dynamics in microfluidic devices, examining hard polystyrene particles and soft pNIPAM microgels. We uncover a significant deviation in droplet formation time compared to pure systems, similarly to surfactant-laden systems, yet notably, colloids exert minimal impact on droplet size, indicating potential nonlinear effects. The dynamics of neck thinning without colloids agree with the classic pendant drop scaling laws, while particle presence replaces traditional viscous and inertial-viscous regimes with a single power law, suggesting an elastic behavior driven by soft particle interactions.

DOI: 10.1103/PhysRevFluids.9.L052201

Introduction. Liquid dripping and droplet detachment is a phenomenon of great interest in various fields. Precise control of droplet formation is fundamental for several scientific and industrial applications, from inkjet printing to material synthesis and targeted drug delivery [1,2]. In such processes, clear understanding of the pinch-off dynamics is key to finely tune the final droplet sizes.

Stemming from the initial works of Egger [3] and Papageorgiou [4], scaling theories of pinch off have been developed over the past decades with the aim of understanding and describing the force balance applied on the droplet neck during the thinning stage [5–7]. In a pendant drop configuration, the thinning dynamics leading to the final pinch off evolve over time according to the dominant force balance. For a Newtonian fluid, if inertia dominates, the thinning occurs in the inertial regime (type I) [8–10]. In this regime, the balance between inertial and capillary forces leads to $h_{\min} \sim \tau^{2/3}$, where $h_{\min}$ is the minimum radius of the liquid filament and τ is the pinch-off time. Similarly, if viscous effects dominate, thinning occurs in the viscous regime (type V) [4]. In this case, the balance between viscous and capillary forces controls the dynamics, leading to a different scaling, $h_{\min} \sim (K_V/Oh)\tau$, where K_V is a constant (i.e., $K_V = 0.0709$ for a pendant drop in air), and Oh is the Ohnesorge number. Independently of the initial thinning regime (i.e., type I or V), when $h_{\min}$ tends to zero, the pinch off always occurs in the inertial-viscous regime (type IV), where the balance between inertial, viscous and capillary forces yields $h_{\min} = (K_{IV}/Oh)\tau$, with the constant $K_{IV} = 0.0304$ for a pendant drop in air [3,5]. In general, when both phases, i.e., drop and surrounding fluid, are Newtonian, the scaling laws described above were found to always hold, with only a modification in the prefactors K_V and K_{IV} depending on the viscosity ratio of the two phases [11,12]. Finally, for

*l.chagot@ucl.ac.uk

$Oh < 1$, it was shown that the pinch-off process always goes through the three different regimes, following the route I → V → IV [5,6,13].

In the presence of surface active agents, the self-similar character of the thinning dynamics still holds. However, additional stress components at the interface can slow down the dynamics. For instance, for surfactant-laden unconfined filaments, Marangoni stresses induced by gradients of the local interfacial tension were found to slow down the thinning dynamics [6,14,15]. This phenomenon suggests a route to tune the droplet formation in different configurations such as microfluidic channels, which could prove advantageous from a processing standpoint. Microfluidic systems offer a valuable route to quickly obtain droplets with monodisperse sizes at constant formation rates [16]. In these devices, the dripping regime is typically used to ensure regular droplet generation, while addition of surfactants enables tuning of the droplet formation time [17–19]. For these systems, the decrease in formation time is attributed to a reduction in interfacial tension. This, in turn, leads to a decrease in the final droplet size, a factor that may be undesirable depending on the specific application.

The use of colloidal particles as interface stabilisers has emerged as an alternative to surfactants [20–22]. The possibility of tuning particle properties to obtain targeted functionalities [23], as well as the higher flexibility to address sustainability issues posed by surfactants, makes particle-stabilized interfaces extremely attractive for the development of advanced materials [24,25]. Unlike surfactant molecules, solid particles can irreversibly adsorb at the interface, yielding complex interfacial properties [26,27]. Adsorbed particles can alter the macroscopic, or apparent, interfacial tension and simultaneously induce interfacial viscoelastic responses that can affect the droplet formation dynamics. For unconfined drops, few studies have found that interfacial rheology effects, induced by particles interfacial networks, can modify the pinch-off dynamics by altering the balance between viscous and capillary forces (regime V) [7,28,29]. Nonetheless, a clear understanding of the role of interfacial rheology and specific colloidal particle attributes on these dynamics is still missing. Additionally, the applicability of the scaling laws described above when the drop is confined and surrounded by convective flows, as in a microfluidic device, has not been directly investigated.

In this Letter, we investigate experimentally the effects of colloidal-laden liquid-liquid interfaces on the droplet pinch-off dynamics in a microfluidic device. We find that the presence of colloidal particles at the interface does not significantly change the final droplet size, even when the interfacial tension is reduced, unlike surfactants. The droplet formation time, however is affected. Using the scaling theories, the analysis of the droplet neck thinning shows a clear modification of the pinch-off dynamics, implying a transition toward a non-Newtonian behavior as the particle concentration increases. Overall, the results indicate that the scaling behavior is dictated by particle interactions, rather than the properties of individual particles.

Results. All experiments were performed in a T-junction microchannel. The dispersed phase (water) was introduced through the side channel with a flow rate Q_d of 50 μL min^{-1} and the continuous phase (dodecane) through the main channel with a flow rate Q_c of 100 μL min^{-1} (see the Supplemental Material [30]), as shown in Fig. 1(a). To investigate the effect of different particle attributes, we employed two sets of colloids, i.e., hard colloids (polystyrene particles - PS) and soft colloids (pNIPAM microgels - MG), with a similar radius of respectively 181 nm and 174 nm (see the Supplemental Material [30] for details on colloids synthesis and properties). Both sets of colloidal particles were added in the aqueous phase at different concentrations. The characteristic Péclet number [$Pe \equiv U r_c/\mathcal{D}$, where $U = (Q_d + Q_c)/A_j$ is the superficial velocity calculated at the channel junction—refer to Fig. S1 for characteristic sizes—, r_c is the colloids radius, and $\mathcal{D} = k_b T/6\pi\mu_w r_c$ is the brownian diffusion coefficient] for both sets of colloids is $1.3{\cdot}10^4$ and $1.2{\cdot}10^4$ for the PS and MG, respectively. This indicates that convection dominates the transport of colloids and we expect particle attachment to be facilitated by the strong kinetic energy, which pushes the particles in the proximity of the interface. All the stages of the droplet generation, from expansion to detachment, were recorded with a high-speed camera (Phantom VEO 1310) at a frequency of 20 kHz and average spatial resolution of 2.3 μm [Fig. 1(a)]. We

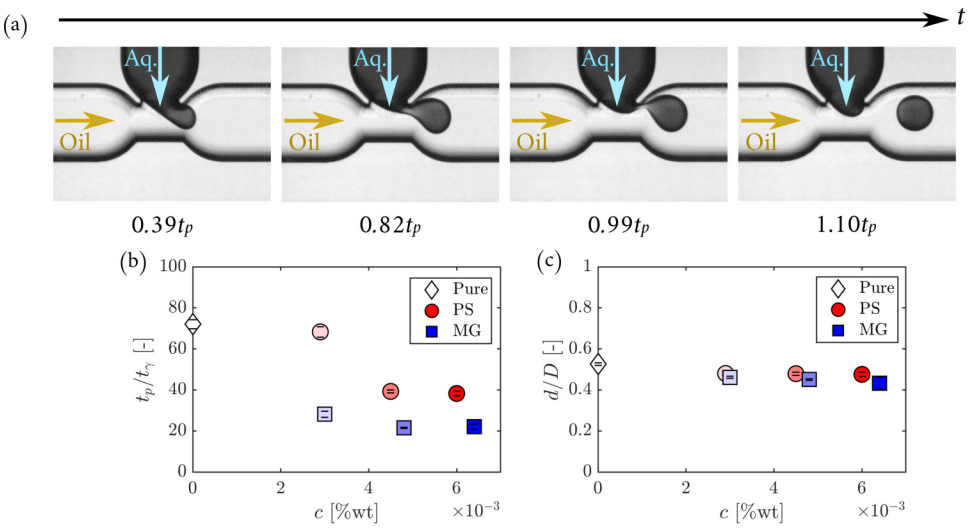

FIG. 1. (a) Pinch-off dynamics of a colloid-laden droplet of water (PS 0.60%wt) in dodecane inside a T-junction microchannel; (b) Evolution of the time to pinch-off (t_p) normalized by the capillary time (t_γ) for different concentrations of colloids; (c) Evolution of the droplet diameter (d) normalized by the channel diameter (D) for different concentrations of colloids. In both graphics, squares are used for pNIPAM microgels (MG) and circles for polystyrene particles (PS). The error bars, within the symbols, show the standard deviation.

first present the effect of the colloids on the global characteristics of the droplet formation, e.g., formation time and droplet size. Figure 1(b) shows the effect of particle concentration on the average formation time of the droplets, or the time to pinch off, t_p, scaled by the capillary time $t_\gamma = \sqrt{\rho_d h_0^3/\gamma}$, where ρ_d, h_0, and γ are respectively the density of the liquid droplet, the neck radius when the thinning starts, and the interfacial tension. For low concentrations of PS ($c = 0.29$%wt), similarly to the pure case, the pinch off occurs around $70t_\gamma$ implying almost no modification of the system. However, for higher particle concentrations ($c = 0.45$%wt and 0.60%wt) the droplet pinch-off time decreases to values around $40t_\gamma$, highlighting a clear effect on the break-up dynamics when enough PS particles reach the interface. This decrease of t_p can also be observed for a low concentration of MG ($c = 0.30$%wt) showing a tendency of the soft particles to be more easily adsorbed at the interface than the solid particles used in this study. Moreover, the reduction of t_p is significantly enhanced ($t_p \sim 20t_\gamma$) with MG compared to solid particles for equivalent mass concentration ($c = 0.48$%wt, 0.64%wt). Nevertheless, both sets of particles show that, similarly to surfactant molecules [31], colloids can decrease the droplet formation time in microfluidic systems.

In contrast, no significant effects on the average droplet size can be observed. Figure 1(c) shows the formed droplet size (d) normalized by the channel diameter (D) as the concentration of both solid and soft colloids is increased. As expected, due to their similar interfacial tension ($\gamma = 44.0$ mN m^{-1} for the colloid-free case and $\gamma = 40.5$ mN m^{-1} for the PS), no size modifications are observed for the droplet loaded with PS compared to the colloid-free droplet. But surprisingly for the MG, even with a significant decrease of interfacial tension ($\gamma = 16.8$ mN m^{-1}), we observe just a minor impact on the droplet size with a maximal reduction of 15% for the highest concentration ($c = 0.64$%wt). The conservation of droplet size, alongside a decrease in pinch-off time ($t_p/t\gamma$) for colloid-laden droplets, underscores a shift in pinch-off dynamics and the onset of nonlinear phenomena.

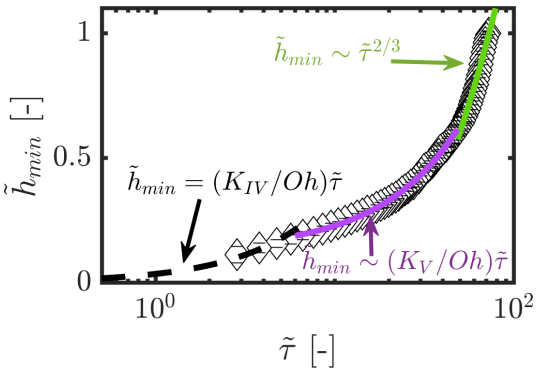

FIG. 2. Evolution of the normalized minimum neck radius with the pinch-off time for the colloid-free case ($Oh = 0.020$). The thinning follows the route I (green line) → V (pink line) → IV (black dashed line), found also for unconfined droplets for $Oh < 1$. The error bars, within the symbols, show the standard deviation.

To quantify the colloids impact on the pinch off, the thinning dynamics for the colloid-free case are first shown as reference. In Fig. 2, we report the evolution of the normalized minimum neck radius $\tilde{h}_{\min} = h_{\min}/h_0$ with the normalized pinch-off time $\tilde{\tau} = \tau/t_\gamma = (t_p - t)/t_\gamma$, where t is the time of the experiment. For the pure case $Oh = \mu_d/\sqrt{\rho_d h_0 \gamma}$ is equal to 0.020. Similarly to pendant drop studies [5,6,13] for $Oh < 1$, the pinch off follows the three classic regimes described in the introduction. Due to the high velocity forced by the flow focusing geometry at the inlet of the T junction, the neck thinning starts with the inertial regime (I) identified by the scaling law $\tilde{h}_{\min} \sim \tilde{\tau}^{2/3}$. Around $\tilde{h}_{\min} \sim 0.5$, the inertia regime is replaced by the viscous regime (V) as the viscous drag increases with the growth of the forming droplet [17], following the linear scaling $\tilde{h}_{\min} \sim (K_V/Oh)\tilde{\tau}$. However, $K_V = 2.02 \times 10^{-4}$ instead of 0.0709, typically found in unconfined configurations for gas/liquid systems [4,5]. The persistence of the power-law index highlights that the self-similarity of the neck thinning is preserved also in confined geometries, with a difference only in the prefactor K_V, which depends on the viscosity ratio [12] and the geometry of the channel [32]. Finally, the expected inertial-viscous regime (IV) leads the final stage toward the pinch off with $\tilde{h}_{\min} = (K_{IV}/Oh)\tilde{\tau}$, with $K_{IV} = 7.10 \times 10^{-4}$. Similarly to K_V, K_{IV} also depends on the system parameters. This regime transition I → V → IV for colloid-free droplets can be used as a reference for the pinch-off dynamics in our specific geometry, thus helping to highlight the effect of colloids during the droplet formation.

Figure 3 shows the evolution of $\tilde{h}_{\min}$ with $\tilde{\tau}$ for different concentrations of colloids. Given the similarity in interfacial tension, all the PS cases have a similar Ohnesorge number to the colloid-free case, i.e., $Oh = 0.021$. For the lowest PS concentration ($c = 0.29\%$wt), the thinning dynamics recover the same behavior observed for the colloid-free case [Fig. 3(a)], following the transition I → V → IV. This confirms the result observed in Figs. 1(b) and 1(c), where PS particles at this concentration appear to not modify the global characteristics of the droplet formation process. However, for higher concentrations, $c = 0.45 - 0.60\%$wt, even if the film thinning still begins with the inertial regime (I), the viscous regime (V) shifts from a linear behavior toward a power law one ($\tilde{h}_{\min} = 0.060\tilde{\tau}^{0.65}$ for $c = 0.45\%$wt and $\tilde{h}_{\min} = 0.061\tilde{\tau}^{0.64}$ for $c = 0.60\%$wt) [Figs. 3(b) and 3(c)].

A very similar behavior is observed when using the soft microgels. In this case the Ohnesorge number is slightly higher ($Oh = 0.033$), but still lower than one, hence we would expect to observe the transition I → V → IV. As shown in Fig. 3, for all MG concentrations, the initial inertial regime (I) is preserved until $\tilde{h}_{\min} \sim 0.5$, but the classic regimes (V) and (IV) are not recovered anymore. As for the higher concentrations of PS, the final thinning process can be scaled by a new power law: $\tilde{h}_{\min} = \alpha\tilde{\tau}^p$ with $[\alpha, p] = [0.114, 0.60]$, [0.130,0.57], and [0.144,0.54] for $c = 0.30\%$wt, 0.48%wt, and 0.64%wt, respectively. This power law defines a new regime (VP) and highlights that for

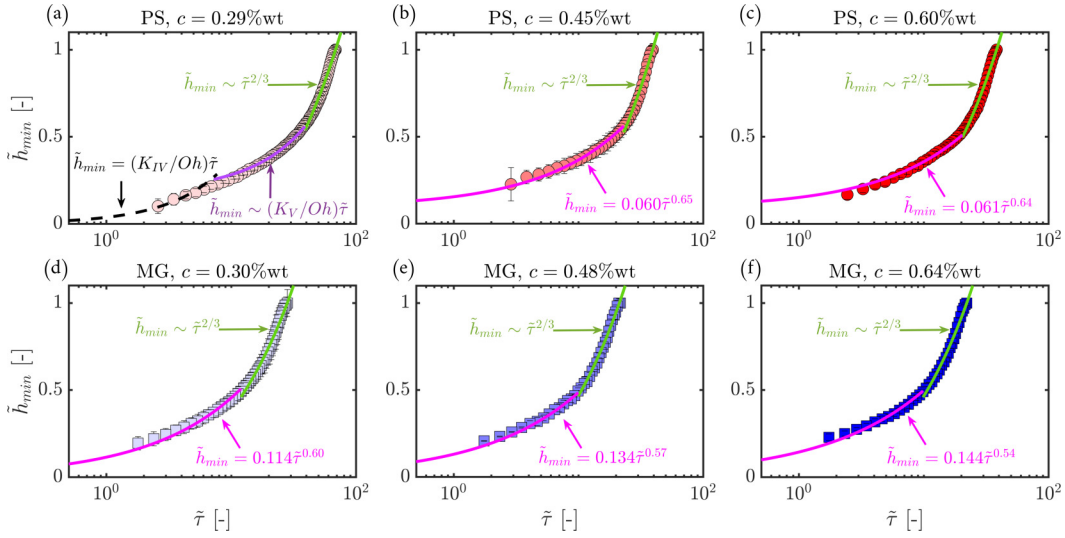

FIG. 3. Evolution of normalized minimum neck radius with the pinch-off time for the PS-laden cases (top row) and the MG-laden cases (bottom row). For PS, $c = 0.29\%$wt, the thinning follows the route I $\rightarrow$ V $\rightarrow$ IV while for all other cases the thinning follows the route I $\rightarrow$ P ($:= \tilde{h}_{\min} = \alpha\tilde{\tau}^{p}$). The error bars, within the symbols, show the standard deviation. All details about the fitting process can be found in Supplemental Material [30].

colloid-laden droplets nonlinear phenomena modify the classic force balance found in Newtonian systems.

The transition to regime (VP) shows similarities with observations of the pinch-off process for non-Newtonian (power-law) fluids, where the power law exponent was found to be linked to the shear-thinning index [33,34]. Despite the Newtonian bulk properties of the fluids, the shift from regimes V and IV to VP serves as a key indicator of the emergence of viscoelastic effects at the interface. In a recent study on the pinch-off dynamics of an unconfined pendant drop loaded with silica particles, the authors reported the onset of nonlinearities in the scaling law of the viscous regime, which they associated to viscoelastic effects of the interface [7]. In our case, due to the strong flow recirculation in the droplet during its formation [31,35], particle transport at the interface can be enhanced compared to larger scales. This transport mechanism can explain the shifts in pinch-off dynamics observed with the increase of particle bulk concentration. The evolution with colloids loading becomes evident when plotting the power law coefficients against particle volume fraction Φ in the bulk, as reported in Fig. 4(a), where the power law index p and the normalized prefactor α/Oh are shown for both PS (circles) and MG (squares) particles. The colloids start to affect the droplet formation dynamics for $\Phi \geqslant 0.0043$, corresponding to $c = 0.45\%$wt for PS particles. The prefactor α/Oh increases linearly with Φ while p decreases linearly, yielding the following generalized scaling:

$$\tilde{h}_{\min} = \alpha(\Phi, Oh)\tilde{\tau}^{p(\Phi)}. \tag{1}$$

The generality of the scaling with Φ, independently of the type of particles, suggests that MG and PS exhibit similar behavior at the interface during the droplet formation process, despite their inherent differences in physical properties. Dilational rheology measurements, as detailed in the Supplemental Material [30], and illustrated in Fig. 4(b), provide further evidence supporting the analogy between these two sets of colloids. Figure 4(b) shows the evolution of both the elastic (E') and viscous (E'') dilational moduli of MG and PS monolayers as a function of the apparent interfacial pressure Π_a. In these measurements, an increase of Π_a is equivalent to an increase of

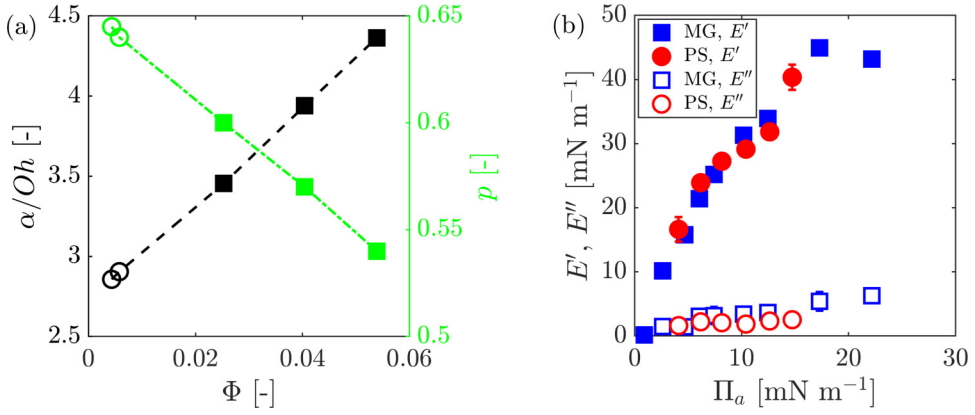

FIG. 4. (a) Evolution of the coefficients α and p of the regime (P) with the solid volume fraction Φ. (b) Evolution of the elastic and viscous moduli E' (filled symbols) and E'' (empty symbols) with the interfacial pressure (Π_a). The squares are the PNIPAM microgels (MG) and the circles are the polystyrene spheres (PS).

interfacial particle concentration, c_s. For both particle systems, the elastic component E' dominates over the viscous E'' one, even at low interfacial pressures, showing that elastic effects can be measured even at low interfacial particle concentrations. Interestingly, the values of E' overlap for both colloids indicating similar interparticle interactions. MG networks at intermediate interfacial pressures are typically characterized by "soft" interactions [36], showing a nonmonotonic trend of E', as reported in Fig. 4(b) [37,38]. For hard colloids, soft interactions are also dominant at intermediate c_s for highly charged particles, as a consequence of strong electrostatic repulsions [39], which is the case for the PS particles used in this study (see Table S.2 in the Supplemental Material [30]). Hence, the consistent trends observed in both the interfacial dilational properties and the scaling parameters suggest that the pinch-off dynamics in microfluidic systems are altered in the presence of colloids due to the emergence of elastic effects induced by particles at the interface. Notably, the macroscopic rheological behavior of the particle-laden interface proves to be more crucial than the intrinsic properties of the individual particles.

Conclusions. In this Letter, we investigated the impact of colloids at liquid-liquid interfaces on droplet pinch-off dynamics in microfluidic devices, focusing on hard polystyrene particles (PS) and pNIPAM microgels (MG). We observed a significant deviation in droplet formation time, similarly to surfactant-laden systems, while revealing a major distinction: unlike surfactants, colloids minimally influenced droplet size, hinting at a modification of the formation dynamics beyond the dominance of capillary forces alone. Examining the thinning dynamics of the liquid neck, we noted that in the absence of colloids, the minimum neck radius ($\tilde{h}_{\min}$) adhered to established scaling laws for Newtonian pendant drop pinch off, transitioning from an initial inertial to a viscous regime, and concluding with an inertial-viscous regime (route I $\rightarrow$ V $\rightarrow$ IV). Contrarily, in the presence of colloidal particles, regimes V and IV were replaced by a singular power law, denoted as VP: $\tilde{h}_{\min} = \alpha(\Phi, Oh)\tilde{\tau}^{p(\Phi)}$. This shift suggests an elastic behavior during droplet formation primarily influenced by the soft interactions between the particles and not their intrinsic properties. This result should guide future works toward the study of interfacial rheology of such systems.

Acknowledgments. The authors would like to acknowledge support from the UK Engineering and Physical Sciences Research Council (EPSRC) Programme Grant PREMIERE (Grant No. EP/T000414/1) and The Royal Society (Grant No. IES/R1/221104 - International Exchanges). The authors also acknowledge Dr. Yan Lang for access to experimental facilities to synthetize the colloids used for this work, Yiting He for helping with the synthesis, and Dr. Sepideh Razavi at the University of Oklahoma for access to the instrumentation used for the dilational measurements.

[1] D. Lohse, Fundamental fluid dynamics challenges in inkjet printing, Annu. Rev. Fluid Mech. **54**, 349 (2022).
[2] M. J. Lawrence and G. D. Rees, Microemulsion-based media as novel drug delivery systems, Adv. Drug Delivery Rev. **64**, 175 (2012).
[3] J. Eggers, Universal pinching of 3D axisymmetric free-surface flow, Phys. Rev. Lett. **71**, 3458 (1993).
[4] D. T. Papageorgiou, On the breakup of viscous liquid threads, Phys. Fluids **7**, 1529 (1995).
[5] J. R. Castrejón-Pita, A. A. Castrejón-Pita, S. S. Thete, K. Sambath, I. M. Hutchings, J. Hinch, J. R. Lister, and O. A. Basaran, Plethora of transitions during breakup of liquid filaments, Proc. Natl. Acad. Sci. USA **112**, 4582 (2015).
[6] N. M. Kovalchuk, H. Jenkinson, R. Miller, and M. J. Simmons, Effect of soluble surfactants on pinch-off of moderately viscous drops and satellite size, J. Colloid Interface Sci. **516**, 182 (2018).
[7] P. Bazazi, H. A. Stone, and S. H. Hejazi, Dynamics of droplet pinch-off at emulsified oil-water interfaces: Interplay between interfacial viscoelasticity and capillary forces, Phys. Rev. Lett. **130**, 034001 (2023).
[8] R. F. Day, E. J. Hinch, and J. R. Lister, Self-similar capillary pinchoff of an inviscid fluid, Phys. Rev. Lett. **80**, 704 (1998).
[9] J. B. Keller and M. J. Miksis, Surface tension driven flows, SIAM J. Appl. Math. **43**, 268 (1983).
[10] N. M. Kovalchuk, E. Nowak, and M. J. Simmons, Effect of soluble surfactants on the kinetics of thinning of liquid bridges during drops formation and on size of satellite droplets, Langmuir **32**, 5069 (2016).
[11] X. Jiang, E. Xu, X. Meng, and H. Z. Li, The effect of viscosity ratio on drop pinch-off dynamics in two-fluid flow, J. Ind. Eng. Chem. **91**, 347 (2020).
[12] T. Dong and P. Angeli, Pinching dynamics and multiple droplet generation in partial coalescence, Phys. Rev. Lett. **131**, 104001 (2023).
[13] Y. Li and J. E. Sprittles, Capillary breakup of a liquid bridge: identifying regimes and transitions, J. Fluid Mech. **797**, 29 (2016).
[14] P. M. Kamat, B. W. Wagoner, S. S. Thete, and O. A. Basaran, Role of marangoni stress during breakup of surfactant-covered liquid threads: Reduced rates of thinning and microthread cascades, Phys. Rev. Fluids **3**, 043602 (2018).
[15] R. V. Craster, O. K. Matar, and D. T. Papageorgiou, Pinchoff and satellite formation in surfactant covered viscous threads, Phys. Fluids **14**, 1364 (2002).
[16] L. Yang, N. Kapur, Y. Wang, F. Fiesser, F. Bierbrauer, M. C. Wilson, T. Sabey, and C. D. Bain, Drop-on-demand satellite-free drop formation for precision fluid delivery, Chem. Eng. Sci. **186**, 102 (2018).
[17] E. Roumpea, N. M. Kovalchuk, M. Chinaud, E. Nowak, M. J. Simmons, and P. Angeli, Experimental studies on droplet formation in a flow-focusing microchannel in the presence of surfactants, Chem. Eng. Sci. **195**, 507 (2019).
[18] M. Kalli, L. Chagot, and P. Angeli, Comparison of surfactant mass transfer with drop formation times from dynamic interfacial tension measurements in microchannels, J. Colloid Interface Sci. **605**, 204 (2022).
[19] L. Chagot, C. Quilodrán-Casas, M. Kalli, N. M. Kovalchuk, M. J. Simmons, O. K. Matar, R. Arcucci, and P. Angeli, Surfactant-laden droplet size prediction in a flow-focusing microchannel: a data-driven approach, Lab Chip **22**, 3848 (2022).
[20] J. Frelichowska, M.-A. Bolzinger, and Y. Chevalier, Effects of solid particle content on properties of o/w Pickering emulsions, J. Colloid Interface Sci. **351**, 348 (2010).
[21] Y. Chevalier and M.-A. Bolzinger, Emulsions stabilized with solid nanoparticles: Pickering emulsions, Colloids Surf., A **439**, 23 (2013).
[22] C. Albert, M. Beladjine, N. Tsapis, E. Fattal, F. Agnely, and N. Huang, Pickering emulsions: Preparation processes, key parameters governing their properties and potential for pharmaceutical applications, J. Controlled Release **309**, 302 (2019).
[23] L. Ridel, M.-A. Bolzinger, N. Gilon-Delepine, P.-Y. Dugas, and Y. Chevalier, Pickering emulsions stabilized by charged nanoparticles, Soft Matter **12**, 7564 (2016).
[24] Y. Xia, J. Wu, W. Wei, Y. Du, T. Wan, X. Ma, W. An, A. Guo, C. Miao, H. Yue *et al.*, Exploiting the pliability and lateral mobility of Pickering emulsion for enhanced vaccination, Nat. Mater. **17**, 187 (2018).
[25] H. Jiang, Y. Sheng, and T. Ngai, Pickering emulsions: Versatility of colloidal particles and recent applications, Curr. Opin. Colloid Interface Sci. **49**, 1 (2020), emulsions and Microemulsions.

[26] B. P. Binks, Particles as surfactantssimilarities and differences, Curr. Opin. Colloid Interface Sci. **7**, 21 (2002).
[27] S. Barman and G. F. Christopher, Role of capillarity and microstructure on interfacial viscoelasticity of particle laden interfaces, Journal of Rheology **60**, 35 (2016).
[28] H. Wang and P. Brito-Parada, Deformation dynamics of particle-laden bubbles: The effect of surfactant concentration and particle contact angle, Minerals Engineering **160**, 106706 (2021).
[29] H. Wang and P. R. Brito-Parada, The pinch-off dynamics of bubbles coated by microparticles, J. Colloid Interface Sci. **577**, 337 (2020).
[30] See Supplemental Material at http://link.aps.org/supplemental/10.1103/PhysRevFluids.9.L052201 for that presents the methodology of the experiments, which include Refs. [5,6,13,40–46].
[31] M. Kalli, P. Pico, L. Chagot, L. Kahouadji, S. Shin, J. Chergui, D. Juric, O. Matar, and P. Angeli, Effect of surfactants during drop formation in a microfluidic channel: a combined experimental and computational fluid dynamics approach, J. Fluid Mech. **961**, A15 (2023).
[32] P. Pico, L. Kahouadji, S. Shin, J. Chergui, D. Juric, and O. K. Matar, Drop encapsulation and bubble bursting in surfactant-laden flows in capillary channels, Phys. Rev. Fluids **9**, 034001 (2024).
[33] P. Doshi, R. Suryo, O. E. Yildirim, G. H. McKinley, and O. A. Basaran, Scaling in pinch-off of generalized newtonian fluids, J. Non-Newtonian Fluid Mech. **113**, 1 (2003).
[34] R. Suryo and O. A. Basaran, Local dynamics during pinch-off of liquid threads of power law fluids: Scaling analysis and self-similarity, J. Non-Newtonian Fluid Mech. **138**, 134 (2006).
[35] L. Kahouadji, E. Nowak, N. Kovalchuk, J. Chergui, D. Juric, S. Shin, M. J. Simmons, R. V. Craster, and O. K. Matar, Simulation of immiscible liquid–liquid flows in complex microchannel geometries using a front-tracking scheme, Microfluid. Nanofluid. **22**, 126 (2018).
[36] M. Rey, M. Á. Fernández-Rodríguez, M. Steinacher, L. Scheidegger, K. Geisel, W. Richtering, T. M. Squires, and L. Isa, Isostructural solid-solid phase transition in monolayers of soft core-shell particles at fluid interfaces: structure and mechanics, Soft Matter **12**, 3545 (2016).
[37] F. Pinaud, K. Geisel, P. Massé, B. Catargi, L. Isa, W. Richtering, V. Ravaine, and V. Schmitt, Adsorption of microgels at an oil-water interface: correlation between packing and 2D elasticity, Soft Matter **10**, 6963 (2014).
[38] M.-C. Tatry, E. Laurichesse, J. Vermant, V. Ravaine, and V. Schmitt, Interfacial rheology of model waterair microgels laden interfaces: Effect of cross-linking, J. Colloid Interface Sci. **629**, 288 (2023).
[39] T. Tadros, Electrostatic repulsion and colloid stability, in *Encyclopedia of Colloid and Interface Science*, edited by T. Tadros (Springer,Berlin, Heidelberg, Germany, 2013), p. 363.
[40] G. K. Batchelor, The effect of Brownian motion on the bulk stress in a suspension of spherical particles, J. Fluid Mech. **83**, 97 (1977).
[41] X. Wu, R. Pelton, A. Hamielec, D. Woods, and W. McPhee, The kinetics of poly (*N*-isopropylacrylamide) microgel latex formation, Colloid Polym. Sci. **272**, 467 (1994).
[42] J. Liu, C. S. Y. Tan, Z. Yu, N. Li, C. Abell, and O. A. Scherman, Tough supramolecular polymer networks with extreme stretchability and fast room-temperature self-healing, Adv. Mater. **29**, 1605325 (2017).
[43] M. Mooney, The viscosity of a concentrated suspension of spherical particles, J. Colloid Sci. **6**, 162 (1951).
[44] S. Migliozzi, G. Meridiano, P. Angeli, and L. Mazzei, Investigation of the swollen state of carbopol molecules in non-aqueous solvents through rheological characterization, Soft Matter **16**, 9799 (2020).
[45] S. Thakur and S. Razavi, Particle size and rheology of silica particle networks at the air-water interface, Nanomaterials **13**, 2114 (2023).
[46] S. Razavi, L. M. Hernandez, A. Read, W. L. Vargas, and I. Kretzschmar, Surface tension anomaly observed for chemically-modified janus particles at the air/water interface, J. Colloid Interface Sci. **558**, 95 (2020).